METHOD OF DIMENSIONLESS COEFFICIENTS FOR ANALYSIS OF STRUCTURALLY ORTHOTROPIC PLANE STRUCTURES

PART 2

RICHARD BAREŠ

In Part 1 we have indicated the procedure of analytic investigation for structurally orthotropic plane systems. We have based the analysis on dimensionless parameters K and K^0, for which we gave the definitions as well as their numerical values. These parameters are convenient in determining the deflection $w(x, y)$ due to a line-load $p_{(x)}$, harmonic along the X-direction, as well as the deflection due to the load $p^0_{(x)}$, harmonic along X while uniformly distributed across the width of the system (i.e. in the Y-direction).

Now we shall indicate the procedure for deriving further dimensionless parameters, which will be found suitable in defining and calculating all the stress components (internal forces and moments), at anyone section of the structure.

5. BENDING MOMENTS IN MAIN BEAMS (IN THE X-DIRECTION)

For bending in the X-direction, the moments are given by the second derivative of the deflection $w(x, y)$ as given by Eq. (45), with regard to the relation (9); considering the particular case of a *line load harmonic in the X-direction*, we can write the formula for the bending moments, in main beams as follows

$$M_T = \sum \frac{p_m l^2}{2b\pi m^2} \{K(y)_m + \eta\, \mu(y)_m\} \sin \frac{m\pi x}{l}, \tag{64}$$

where $K(y)_m$ is given by Eq. (46), while $\mu(y)_m$ is a newly introduced dimensionless

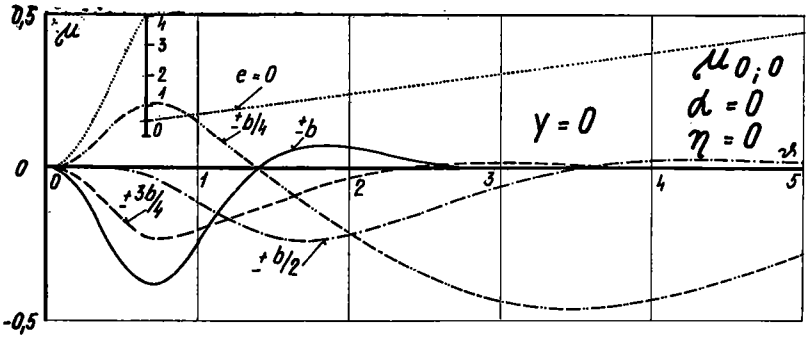

Fig. 27.

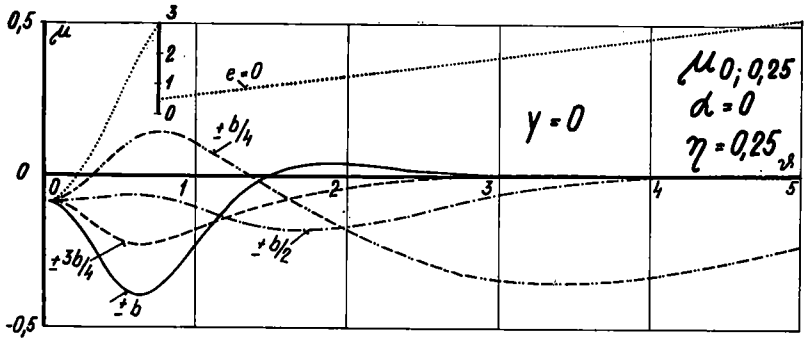

Fig. 28.

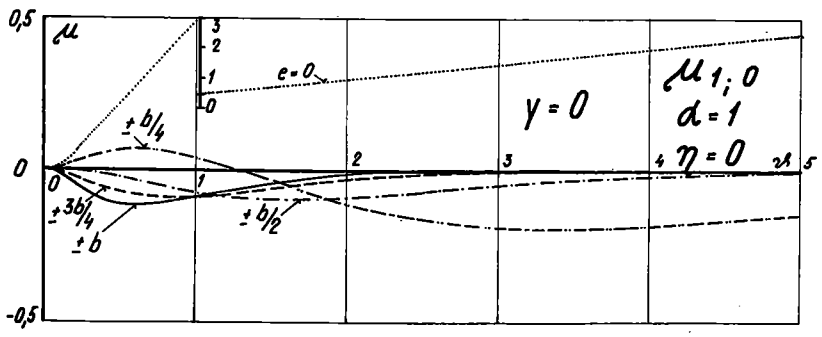

Fig. 29.

parameter. Depending on φ, ψ, ϑ, α and η, it is given by the following expression

$$(65)\quad \mu(y)_m = -\frac{m\vartheta}{\sqrt{[2(1+\varepsilon)]}}\Big[\varepsilon(A'_m M_{\varphi m} + \bar{B}'_m N_{\varphi m}) + \sqrt{(1-\varepsilon^2)}\,(-A'_m N_{\varphi m} + \bar{B}'_m M_{\varphi m}) + \varepsilon(C'_m O_{\varphi m} + \bar{D}'_m P_{\varphi m}) + \sqrt{(1-\varepsilon^2)}\,(C'_m P_{\varphi m} - \bar{D}'_m O_{\varphi m}) + \sqrt{\left(\frac{1+\varepsilon}{1-\varepsilon}\right)} P_{|\varphi-\Psi|m} - O_{|\varphi-\Psi|m}\Big]. \quad ^{1})$$

[1]) For $\eta = 0$ this parameter is the $(2\vartheta^2 m^2 \pi)$-multiple of the original Massonnet parameter [11]; hence

$$[\mu(y)_m]_{\eta=0} = 2\vartheta^2 m^2 \pi\, \mu(y)_m^{\mathrm{MASS}}.$$

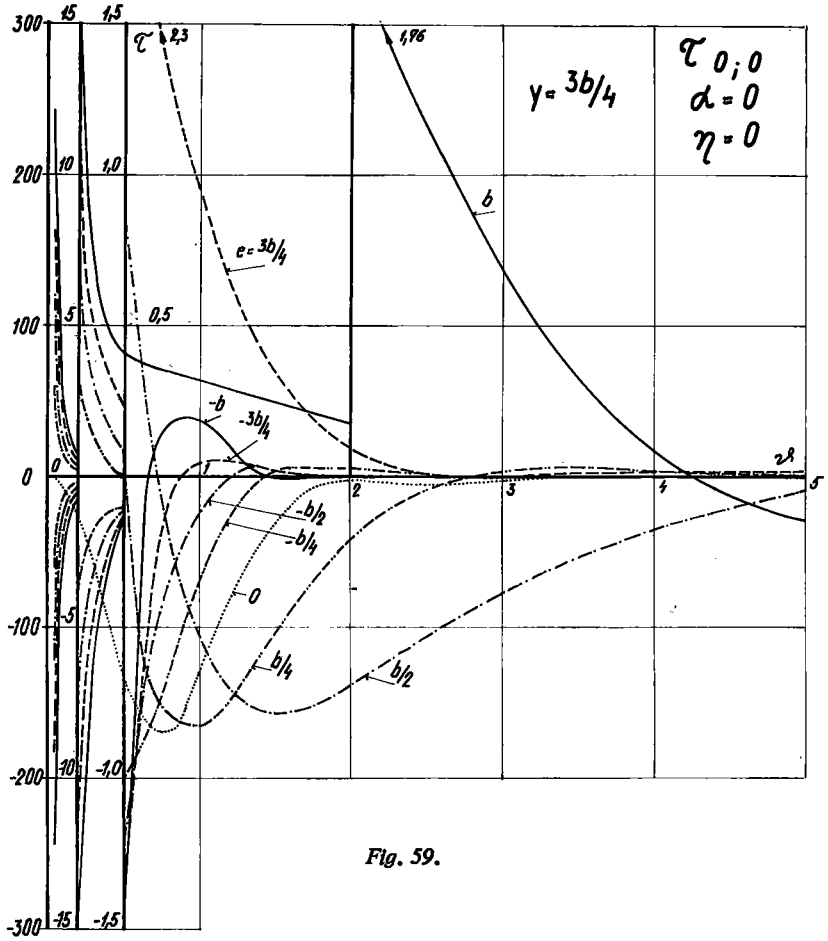
τ 0; 0
α = 0
η = 0
y = 3b/4
τ
2,3
1,96
b
c = 3b/4
0,5
-b
-3b/4
-b/2
-b/4
0
b/4
b/2
ϑ
300
200
100
0
-100
-200
-300
15
1,5
10
1,0
5
-5
-10
-1,0
-15
-1,5
1
2
3
4
5

Fig. 59.

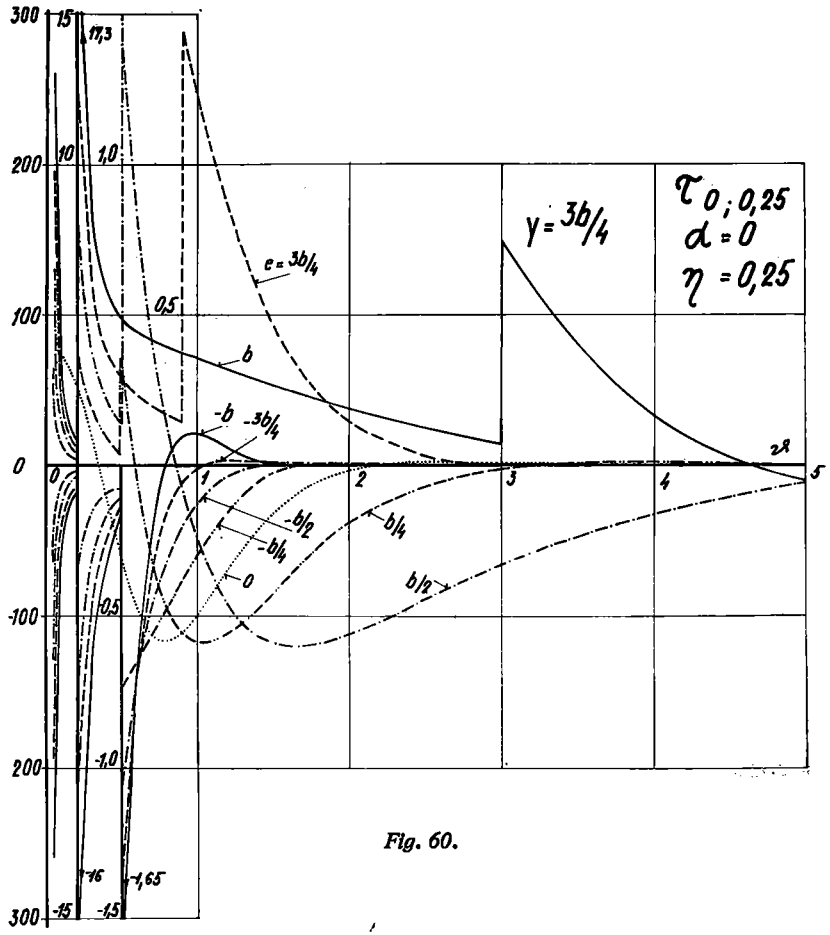
τ 0; 0,25
α = 0
η = 0,25
y = 3b/4
17,3
c = 3b/4
0,5
b
-b
-3b/4
-b/2
-b/4
0
b/4
b/2
ϑ
300
200
100
0
-100
200
300
15
10
1,0
0,5
-1,0
-15
1,6
-1,65
1
2
3
4
5

Fig. 60.

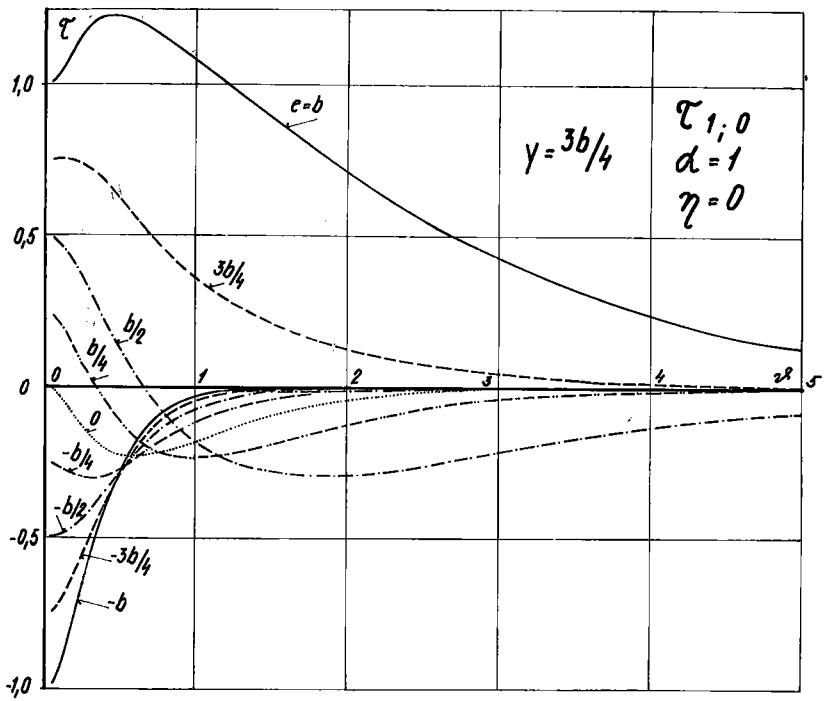
τ
1,0
0,5
0
-0,5
-1,0
e=b
3b/4
b/2
b/4
0
-b/4
-b/2
-3b/4
-b
y = 3b/4
τ 1; 0
α = 1
η = 0
0
1
2
3
4
5

Fig. 61.

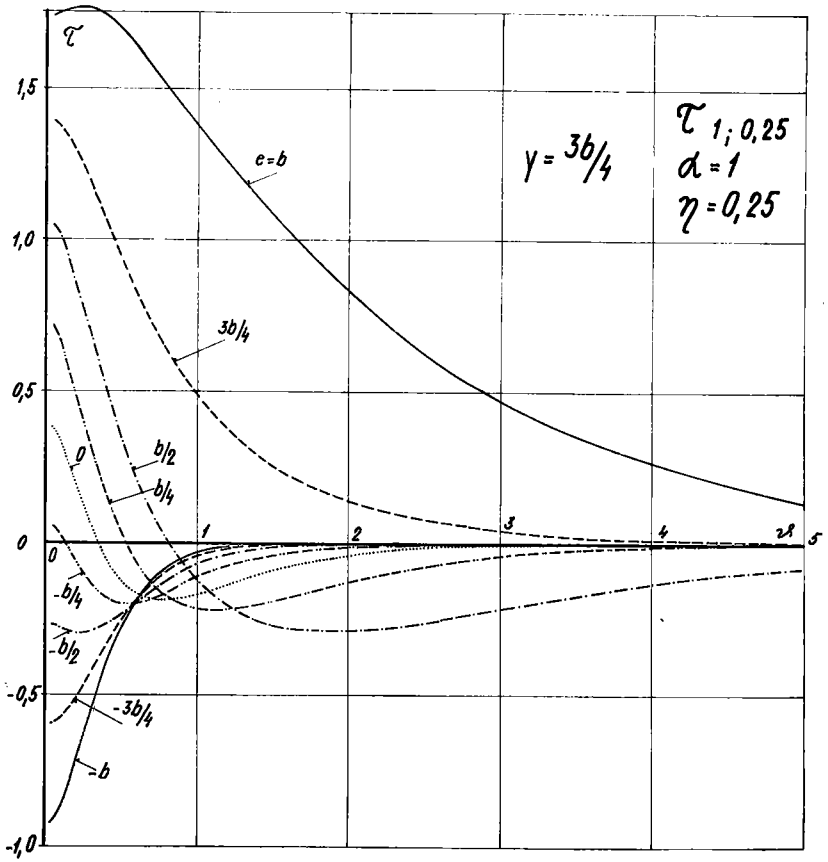
τ
1,5
1,0
0,5
0
-0,5
-1,0
e=b
3b/4
b/2
b/4
0
-b/4
-b/2
-3b/4
-b
y = 3b/4
τ 1; 0,25
α = 1
η = 0,25
0
1
2
3
4
5

Fig. 62.

Fig. 30.

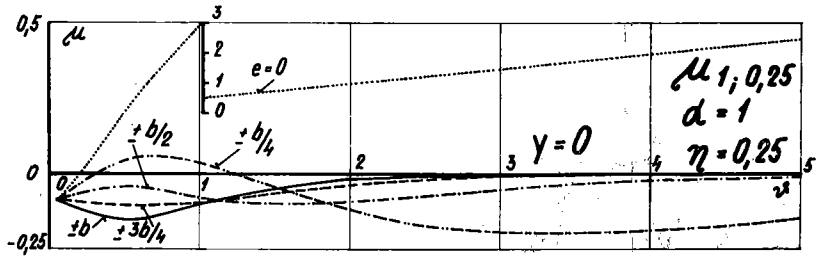

Fig. 31.

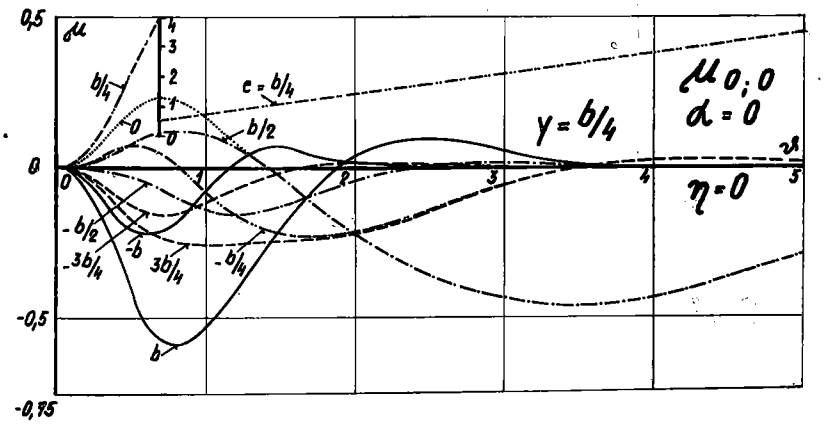

Fig. 32.

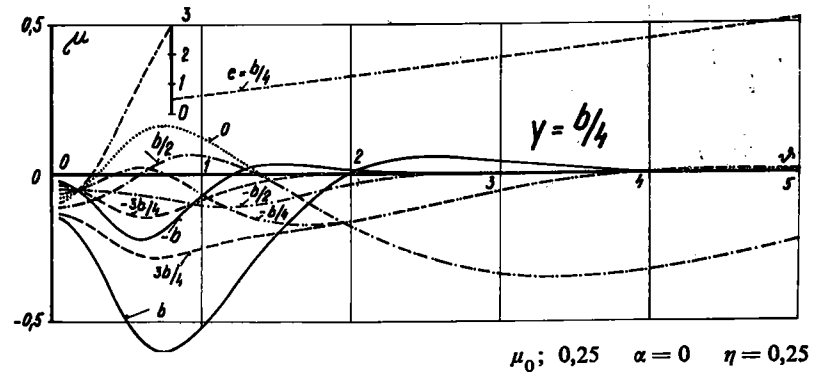

The values of this second dimensionless parameter are shown in the figures 27 to 44, where they are plotted against the values of ϑ for $\alpha = 0$, $\alpha = 1$, and $\eta = 0$ and $\eta = 0{\cdot}25$, for various values of φ and ψ.

In a similar manner, but for *uniformly distributed load in the Y-direction* (while harmonic in the X-direction) we find the bending moments in the main beams to be

$$M_T^0 = \sum \frac{p_m^0 l^2}{\pi^2 m^2} [1 + K^0(y)_m - \eta\, \mu^0(y)_m] \sin \frac{m\pi x}{l}, \tag{66}$$

where $K^0(y)_m$ is given by Eq. (58), and the dimensionless parameter $\mu^0(y)_m$ is given

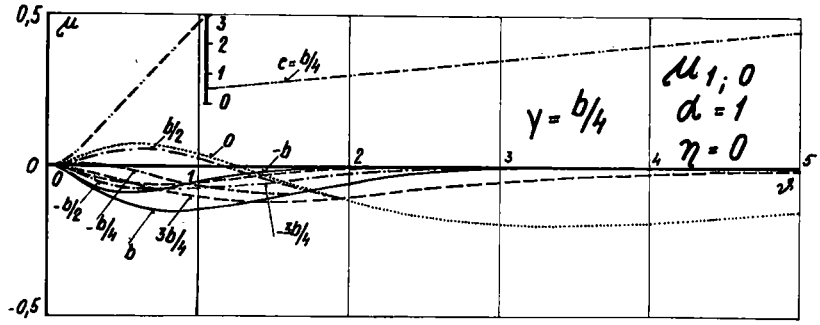

Fig. 33.

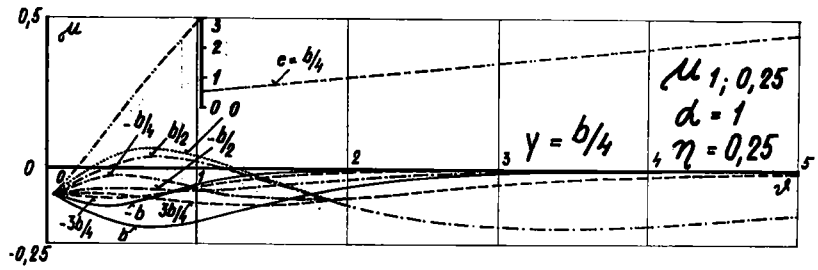

Fig. 34.

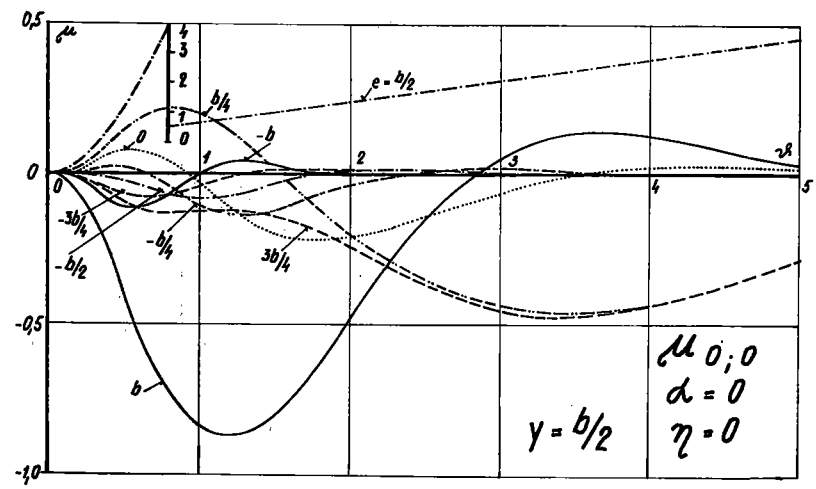

Fig. 35.

by the formula

$$\mu^0(y)_m = \eta\{\varepsilon(A_m^{0\prime}M_{ym} - \bar{B}_m^{0\prime}N_{ym}) - \sqrt{(1-\varepsilon^2)}\,(A_m^{0\prime}N_{ym} + \bar{B}_m^{0\prime}M_{ym}) + \varepsilon(-A_m^{0\prime}O_{ym} + \bar{B}_m^{0\prime}P_{ym}) - \sqrt{(1-\varepsilon^2)}\,(A_m^{0\prime}P_{ym} + \bar{B}_m^{0\prime}O_{ym})\}\,. \tag{67}$$

The variation of $\mu \equiv \mu^0(y)_1$ is illustrated in the figures 45–46, where the values of μ are plotted vers the independent variable ϑ, for $\alpha = 0$, $\alpha = 1$ (while $\eta = 0{\cdot}25$), and for various values of φ.

Fig. 36.

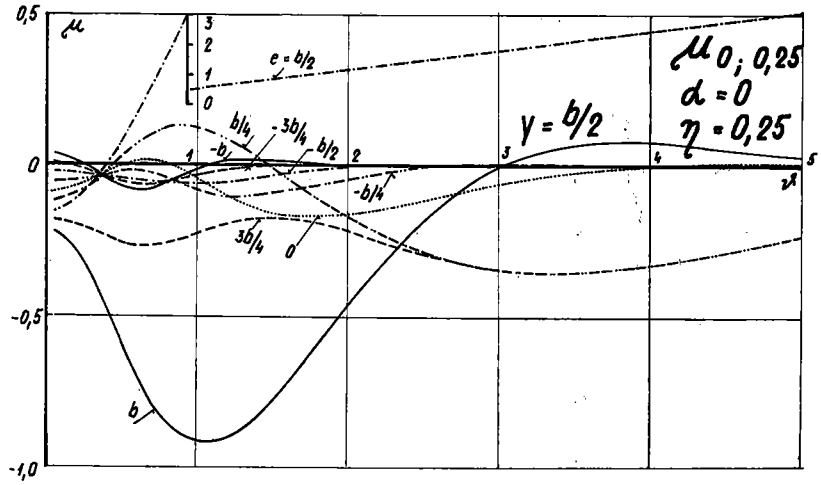

Fig. 37.

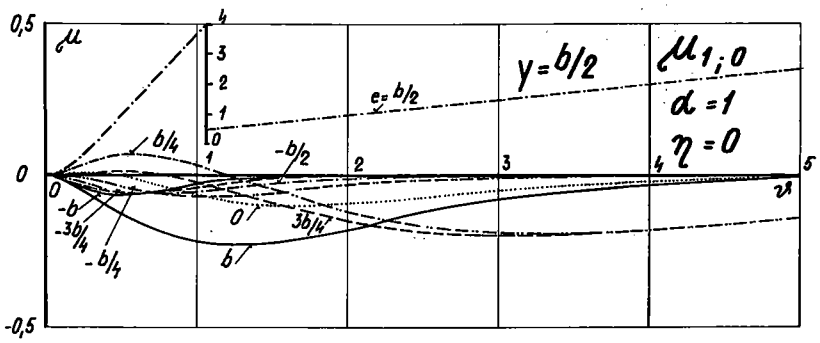

Fig. 38.

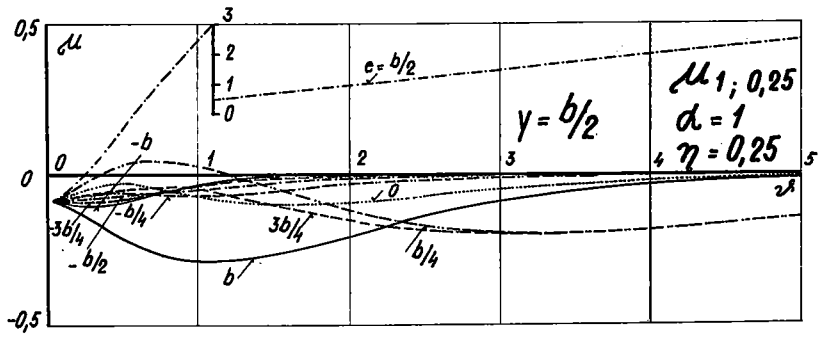

For any other, arbitrary type of load, the pertinent formulae can be obtained by superposition of the individual effects, for instance as shown in [4].

6. TRANSVERSE BENDING MOMENTS (IN THE *Y*-DIRECTION)

For bending in the *Y*-direction, the moments are defined by the corresponding second derivative of the deflection $w(x, y)$ according to (45), and (9); written for the

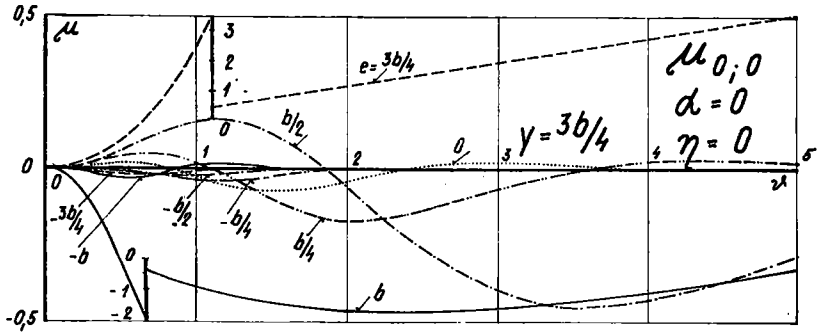

Fig. 39.

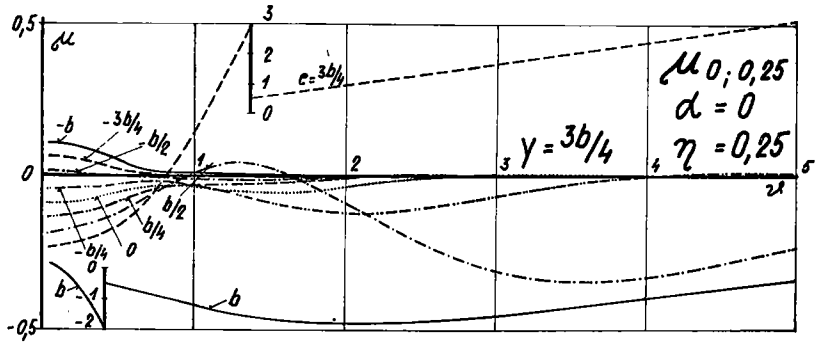

Fig. 40.

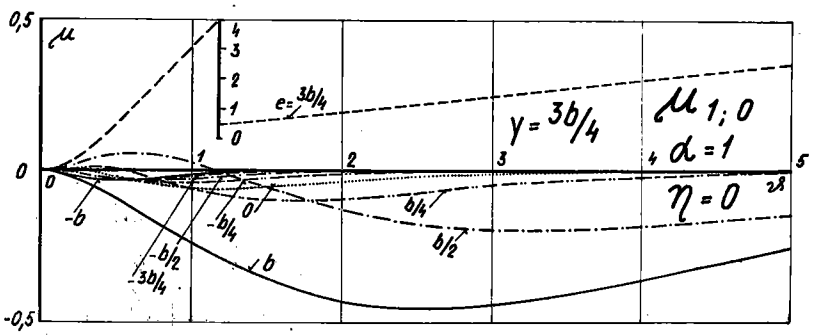

Fig. 41.

particular case of a *line load, harmonically distributed along X*, the formula for transverse bending moments becomes

$$M_P = \sum \frac{p_m b}{2\vartheta^2 m^2 \pi} [\eta K(y)_m + \mu(y)_m] \sin \frac{m\pi x}{l}, \tag{68}$$

where $K(y)_m$ is given by (46), and $\mu(y)_m$ by (65).

For a *loading harmonic along X and uniform along Y* we have, similarly

$$M_P^0 = \sum \frac{p_m^0 b^2}{\vartheta^2 \pi^2 m^2} [\eta - \mu^0(y)_m + \eta K^0(y)_m] \sin \frac{m\pi x}{l} \tag{69}$$

where $K^0(y)_m$ and $\mu^0(y)_m$ are given by the expressions (58) and (67), respectively.

Fig. 42.

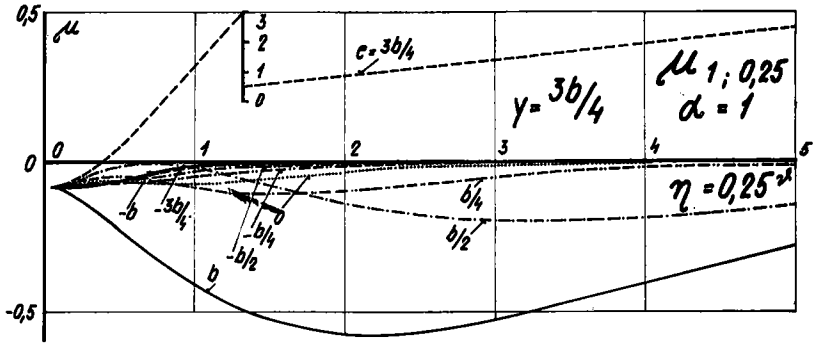

Fig. 43.

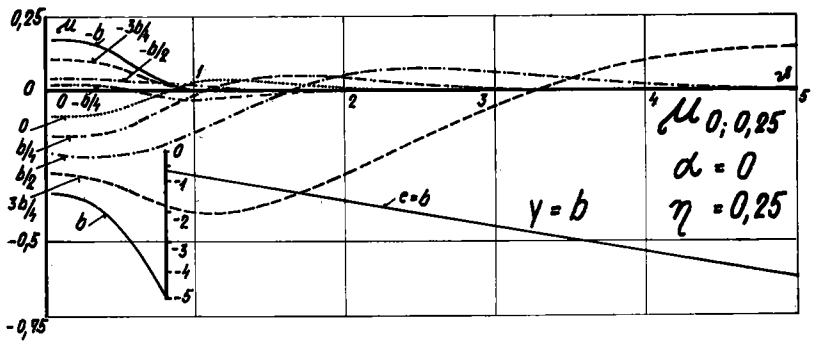

Fig. 44.

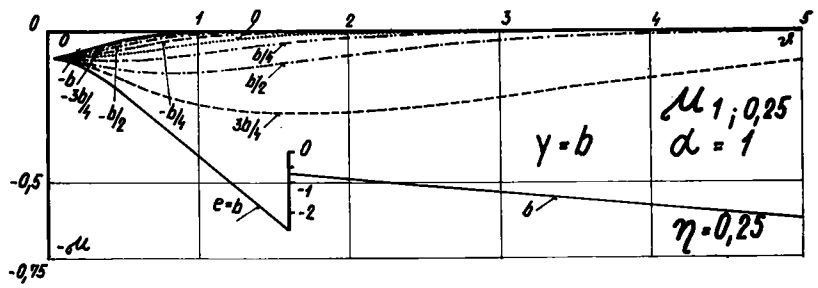

7. TWISTING MOMENTS

The twisting moments which are produced in the main beams and in the cross beams respectively, are for *the case of a harmonic line load* given by the second mixed partial derivative of the deflection $w(x, y)$, as given by Eq. (12).

Considering the difference of the two twisting moments we obtain

$$M_{TP} - M_{PT} = (\gamma_T + \gamma_P) \frac{\partial^2 w}{\partial x \, \partial y}, \tag{70}$$

which is tantamount to

$$(M_{TP} - M_{PT}) = \sum \alpha (1 - \eta) \frac{p_m l}{2\pi m} [\tau(y)_m] \cos \frac{m\pi x}{l}, \tag{71}$$

where

$$(72)\qquad \tau(y)_m = [A'_m M_{\varphi m} + \bar{B}'_m N_{\varphi m}] + \sqrt{\left(\frac{1-\varepsilon}{1+\varepsilon}\right)}[-A'_m N_{\varphi m} + \bar{B}'_m M_{\varphi m}] -$$

$$- [C'_m O_{\varphi m} + \bar{D}'_m P_{\varphi m}] + \sqrt{\left(\frac{1-\varepsilon}{1+\varepsilon}\right)}[-C'_m P_{\varphi m} + \bar{D}'_m O_{\varphi m}] \mp$$

$$\mp \frac{2}{\sqrt{(1-\varepsilon^2)}} P_{|\varphi-\Psi|m}\,.\ ^{1})$$

Fig. 45.

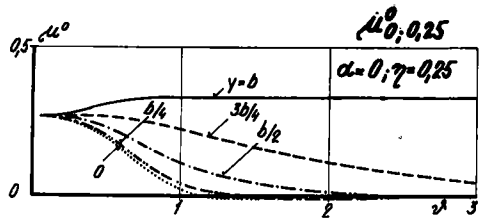

Fig. 46.

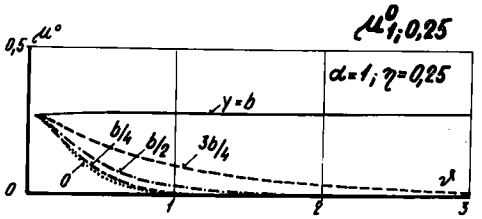

The sign of the last member on the right side differs, depending on the interrelation of ψ and φ. For $\psi > \varphi$ the sign is positive, while for $\psi < \varphi$ the sign becomes negative. The dimensionless parameter $\tau \equiv \tau(y)_1$ is a function of φ, ψ, ϑ, α, and η, and it is represented by the graphs in the figs. 47 to 66, as depending on ϑ. The graphs are plotted for $\alpha = 0$, $\alpha = 1$, $\eta = 0$, and $\eta = 0{\cdot}25$.

The twisting moments in the equivalent slab are, for the main and for the lateral directions respectively, given by the formulae

$$(73)\qquad M_{TP} = \frac{\gamma_T}{\gamma_T + \gamma_P}(M_{TP} - M_{PT})$$

$$M_{PT} = \frac{\gamma_P}{\gamma_T + \gamma_P}(M_{TP} - M_{PT})\,.$$

[1]) For $\eta = 0$ this parameter is the $(4/\alpha)$-multiple of the parameter due originally to Bareš [8, 164], that is we have

$$[\tau(y)_m]_{\eta=0} = (4/\alpha)\,\tau(y)_m^{\mathrm{BAR}}\,.$$

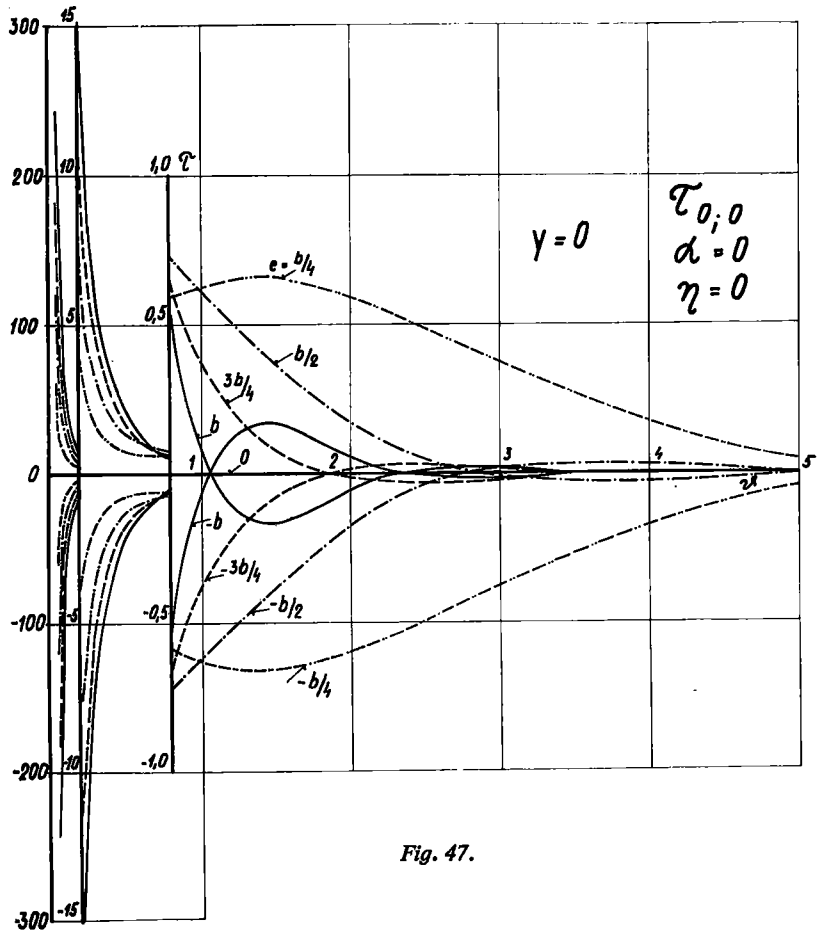
300
200
100
0
-100
-200
-300
15
10
5
-5
-10
-15
1,0 τ
0,5
-0,5
-1,0
e = b/4
b/2
3b/4
b
0
1
2
3
4
5
2λ
-b
-3b/4
-b/2
-b/4
γ = 0
τ 0; 0
α = 0
η = 0

Fig. 47.

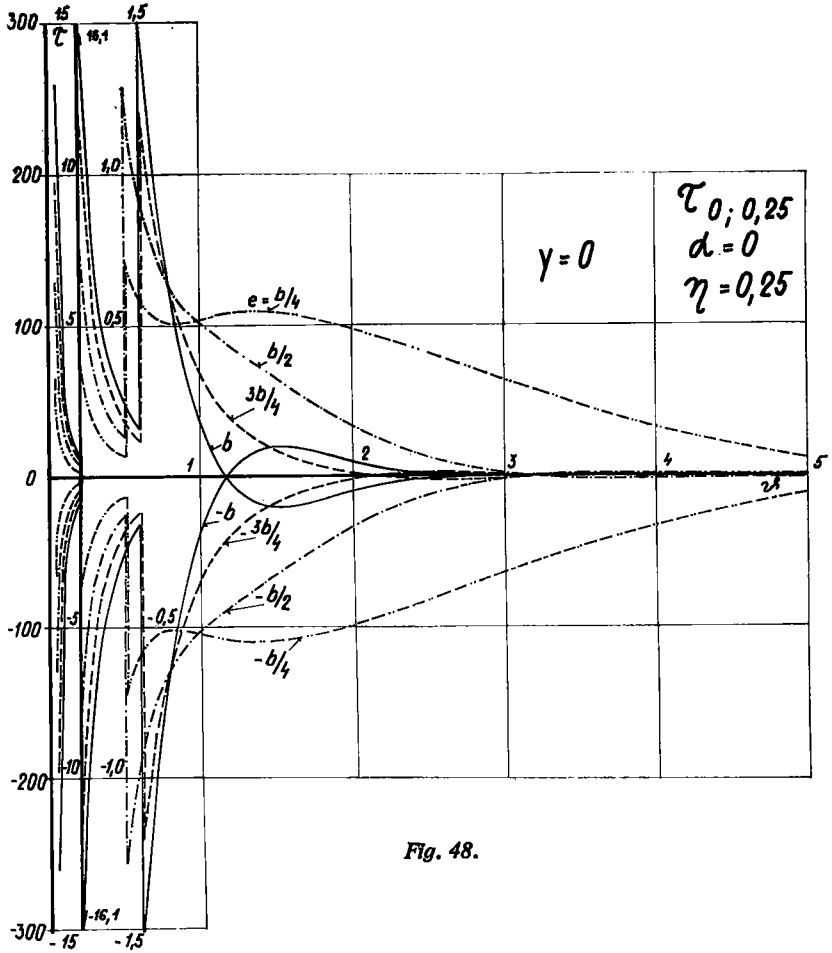
300
200
100
0
-100
-200
-300
15
τ
16,1
1,5
10
1,0
5
0,5
-5
-0,5
-10
-1,0
-16,1
-15
-1,5
e = b/4
b/2
3b/4
b
1
2
3
4
5
2λ
-b
-3b/4
-b/2
-b/4
γ = 0
τ 0; 0,25
α = 0
η = 0,25

Fig. 48.

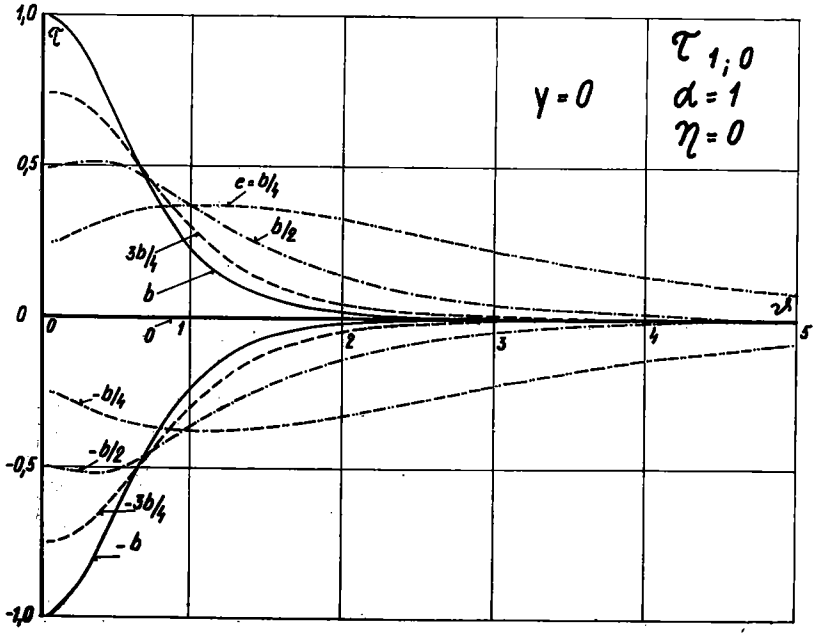
1,0
τ
0,5
0
-0,5
-1,0
0
0
1
2
3
4
5
x
y = 0
τ 1; 0
α = 1
η = 0
e = b/4
b/2
3b/4
b
-b/4
-b/2
-3b/4
-b

Fig. 49.

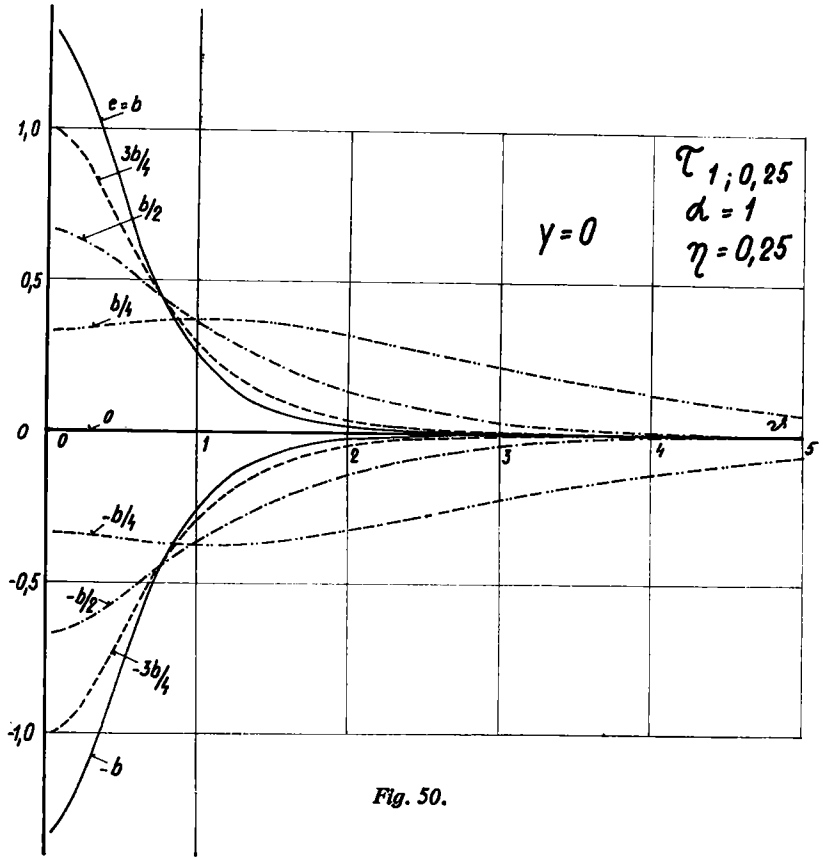
1,0
0,5
0
-0,5
-1,0
0
0
1
2
3
4
5
x
y = 0
τ 1; 0,25
α = 1
η = 0,25
e = b
3b/4
b/2
b/4
-b/4
-b/2
-3b/4
-b

Fig. 50.

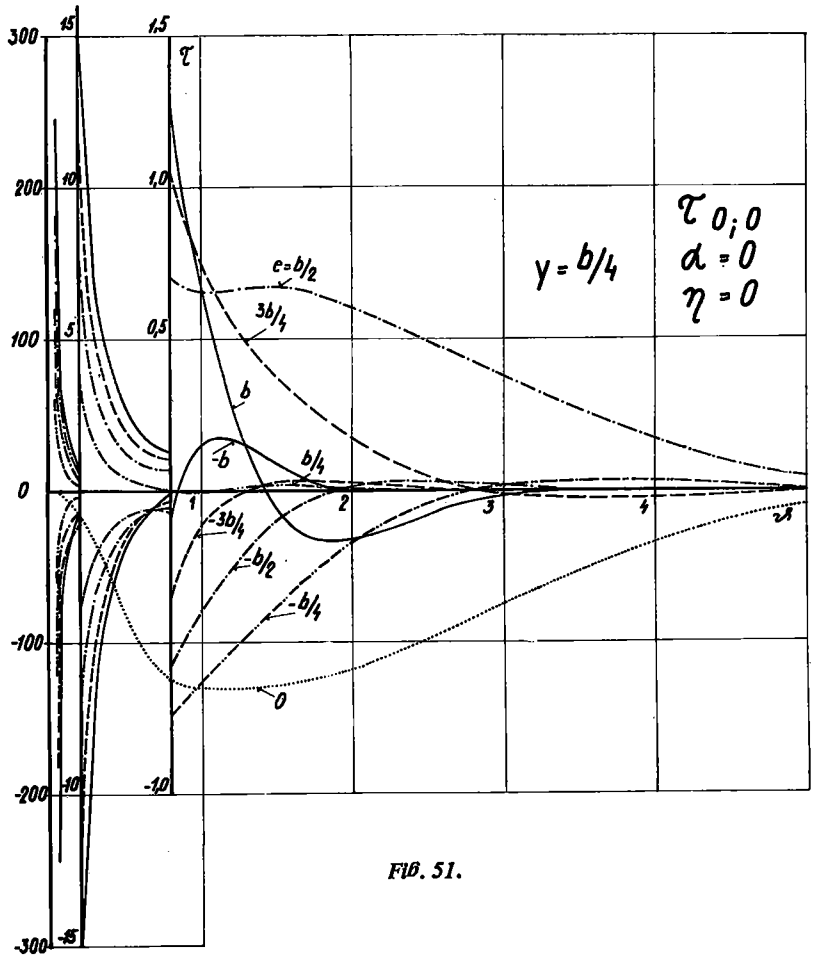
τ
y = b/4
τ 0; 0
α = 0
η = 0
e = b/2
3b/4
b
b/4
-b
-3b/4
-b/2
-b/4
0

Фиг. 51.

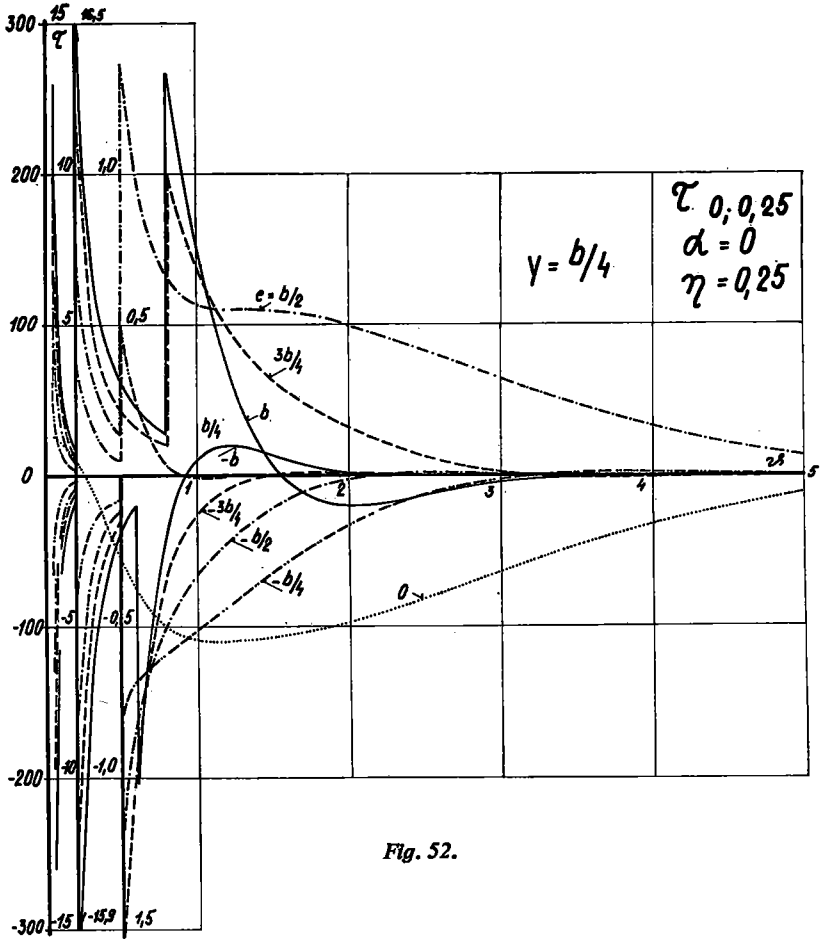
τ
y = b/4
τ 0; 0,25
α = 0
η = 0,25
e = b/2
3b/4
b
b/4
-b
-3b/4
-b/2
-b/4
0

Fig. 52.

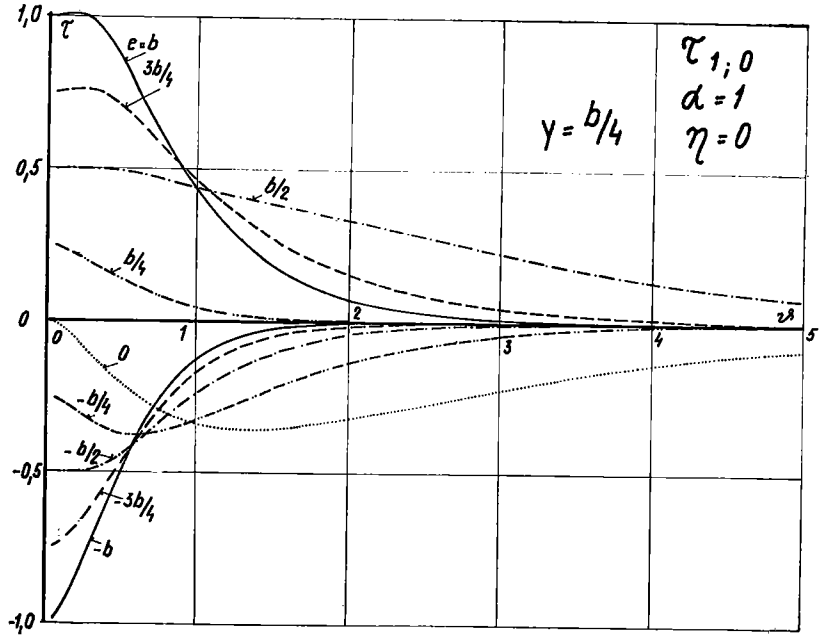
1,0
0,5
0
-0,5
-1,0
τ
e=b
3b/4
b/2
b/4
0
-b/4
-b/2
-3b/4
-b
y = b/4
τ 1; 0
α = 1
η = 0
0
1
2
3
4
5
x̄

Fig. 53.

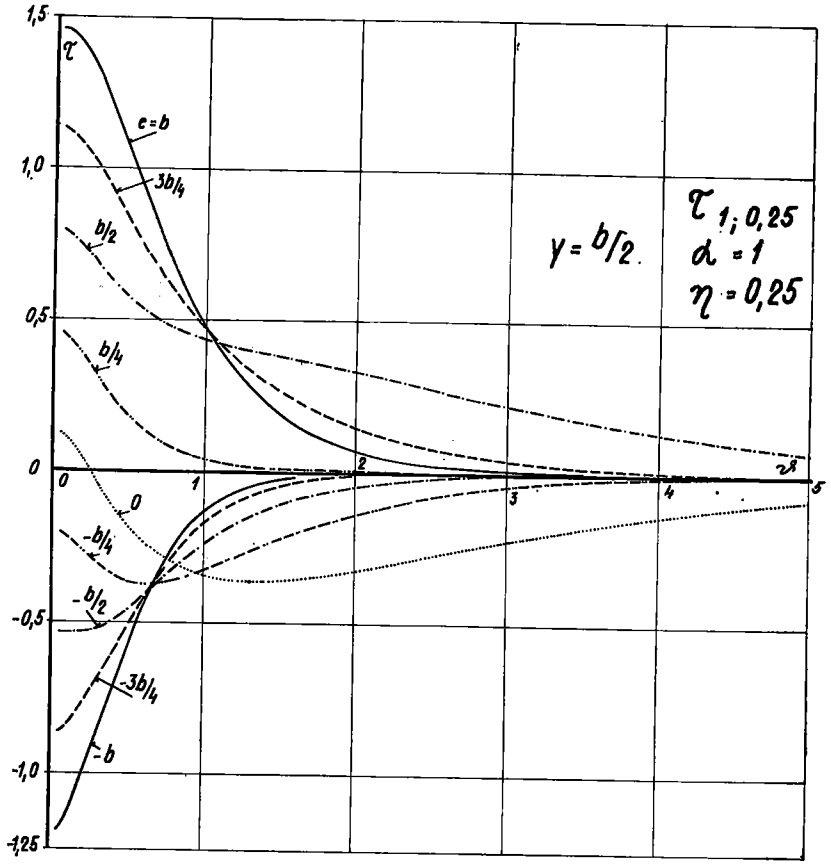
1,5
1,0
0,5
0
-0,5
-1,0
-1,25
τ
e=b
3b/4
b/2
b/4
0
-b/4
-b/2
-3b/4
-b
y = b/2
τ 1; 0,25
α = 1
η = 0,25
0
1
2
3
4
5
x̄

Fig. 54.

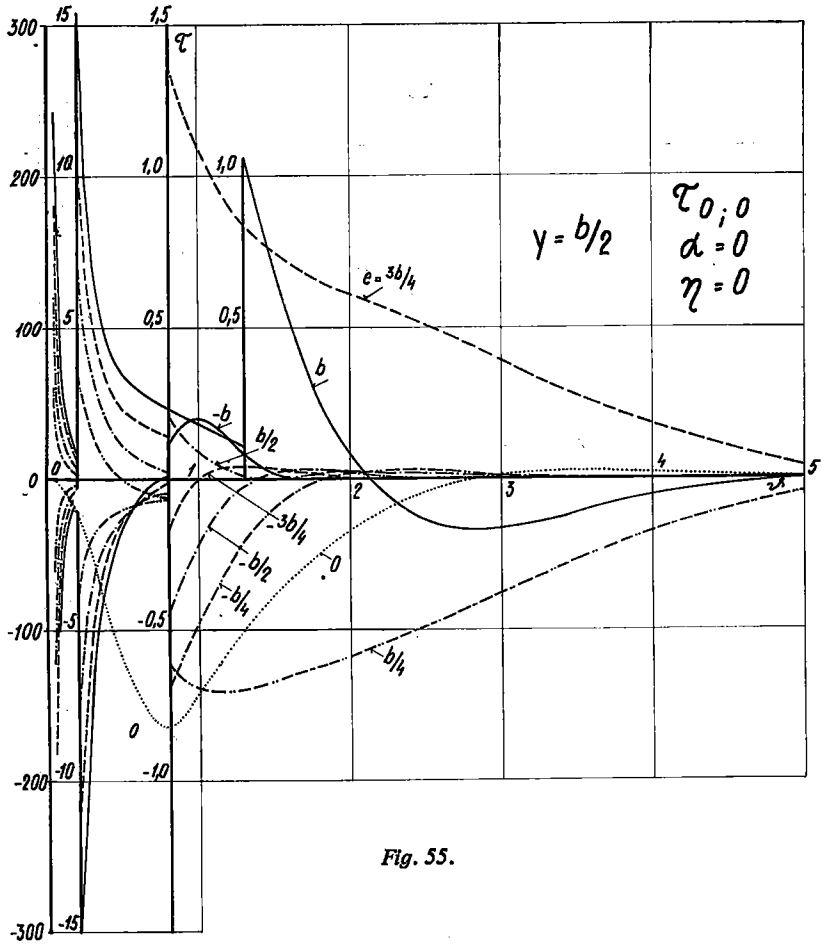
τ
y = b/2
τ 0 ; 0
α = 0
η = 0
e = 3b/4
b
b/2
-b
-3b/4
-b/2
-b/4
0
300
200
100
0
-100
-200
-300
15
10
5
0
-5
-10
-15
1,5
1,0
0,5
-0,5
-1,0
1
2
3
4
5
x

Fig. 55.

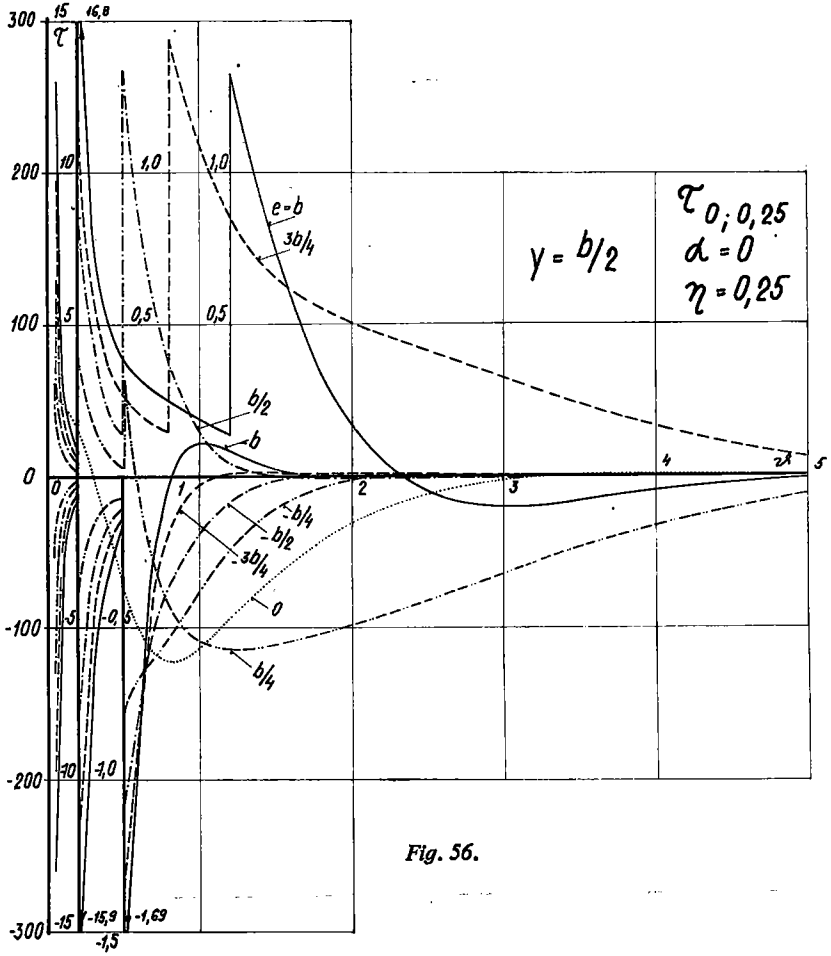
τ
y = b/2
τ 0 ; 0,25
α = 0
η = 0,25
e = b
3b/4
b/2
b
-b/4
-b/2
-3b/4
0
-b/4
300
200
100
0
-100
-200
-300
15
16,8
10
5
0
-5
-10
-15
-15,9
-1,69
-1,5
1,0
0,5
-0,5
-1,0
1
2
3
4
5
x

Fig. 56.

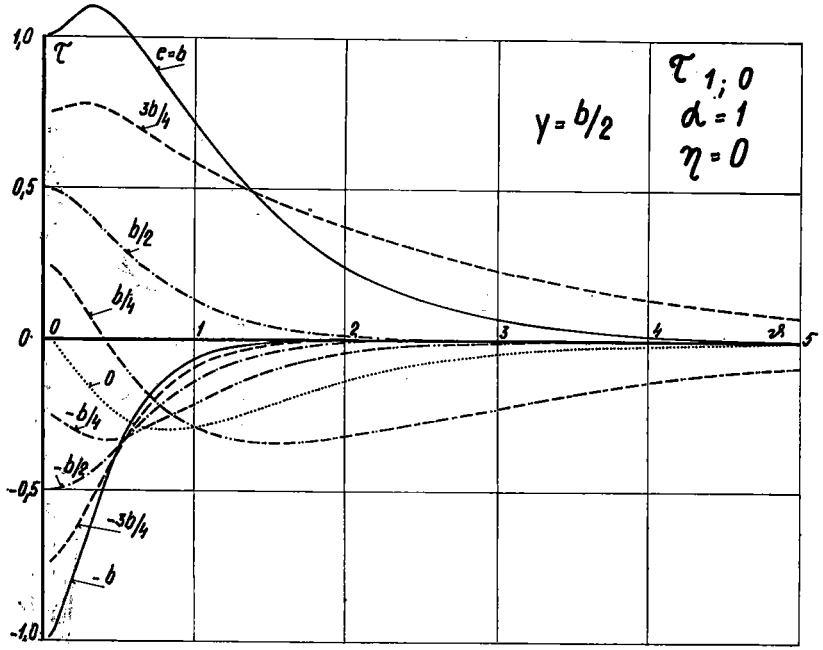
τ
1,0
0,5
0
-0,5
-1,0
c=b
3b/4
b/2
b/4
0
-b/4
-b/2
-3b/4
-b
y = b/2
τ 1; 0
α = 1
η = 0
0
1
2
3
4
ξ
5

Fig. 57.

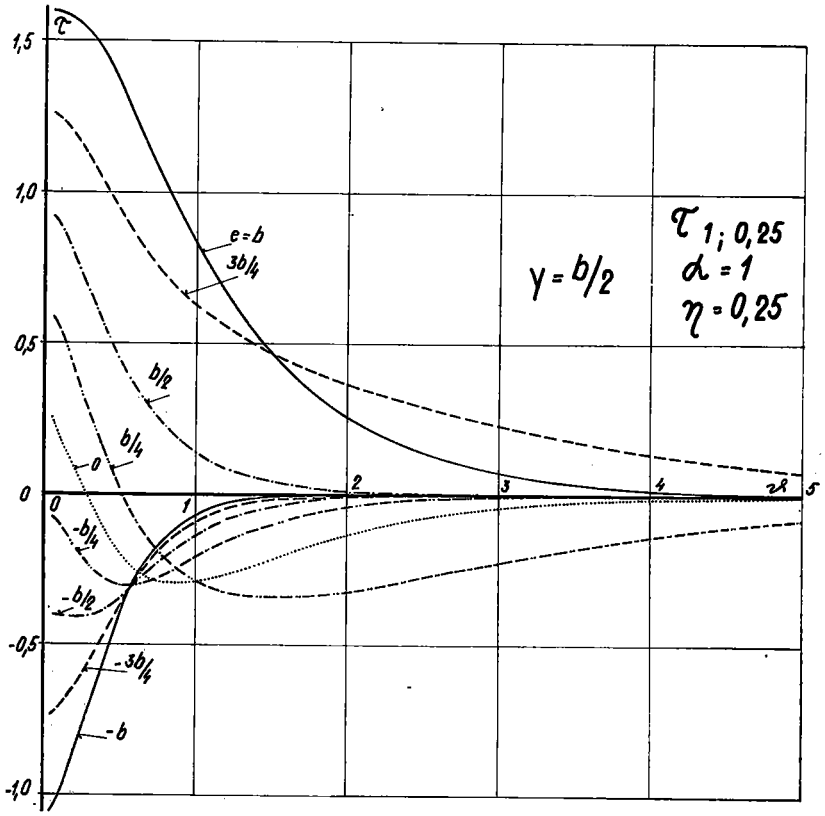
τ
1,5
1,0
0,5
0
-0,5
-1,0
c=b
3b/4
b/2
b/4
0
-b/4
-b/2
-3b/4
-b
y = b/2
τ 1; 0,25
α = 1
η = 0,25
0
1
2
3
4
ξ
5

Fig. 58.

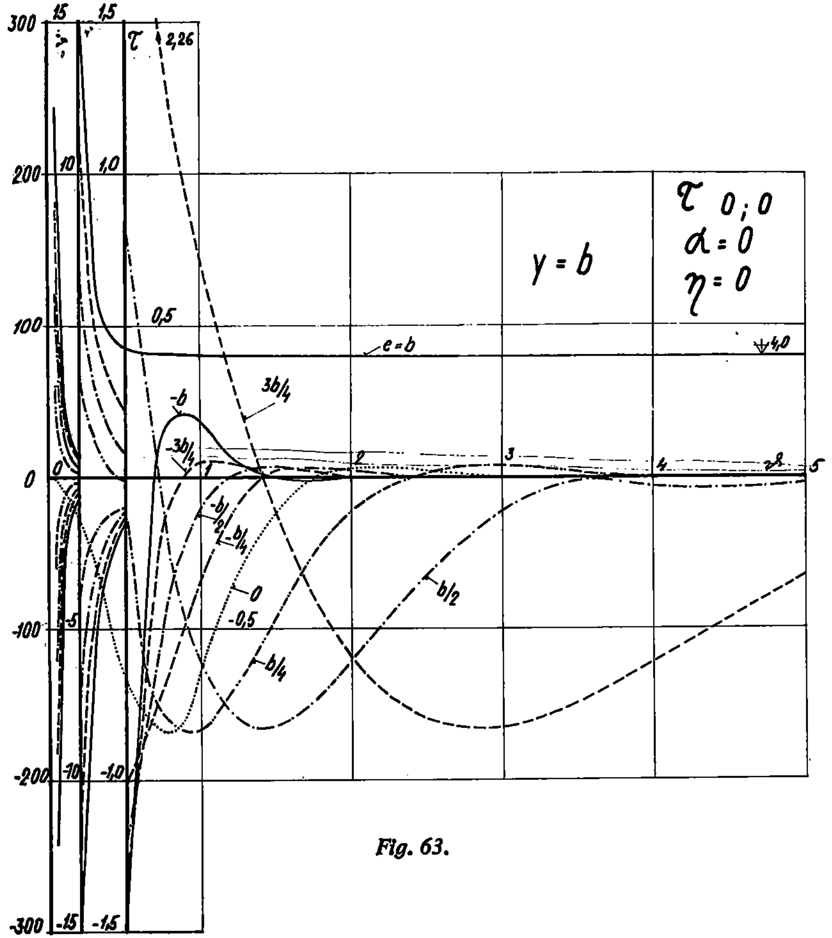
y = b
τ 0 ; 0
α = 0
η = 0
e = b
3b/4
-b
-3b/4
-b/2
-b/4
0
-0,5
b/4
b/2
0,5
1,0
1,5
2,26
4,0

Fig. 63.

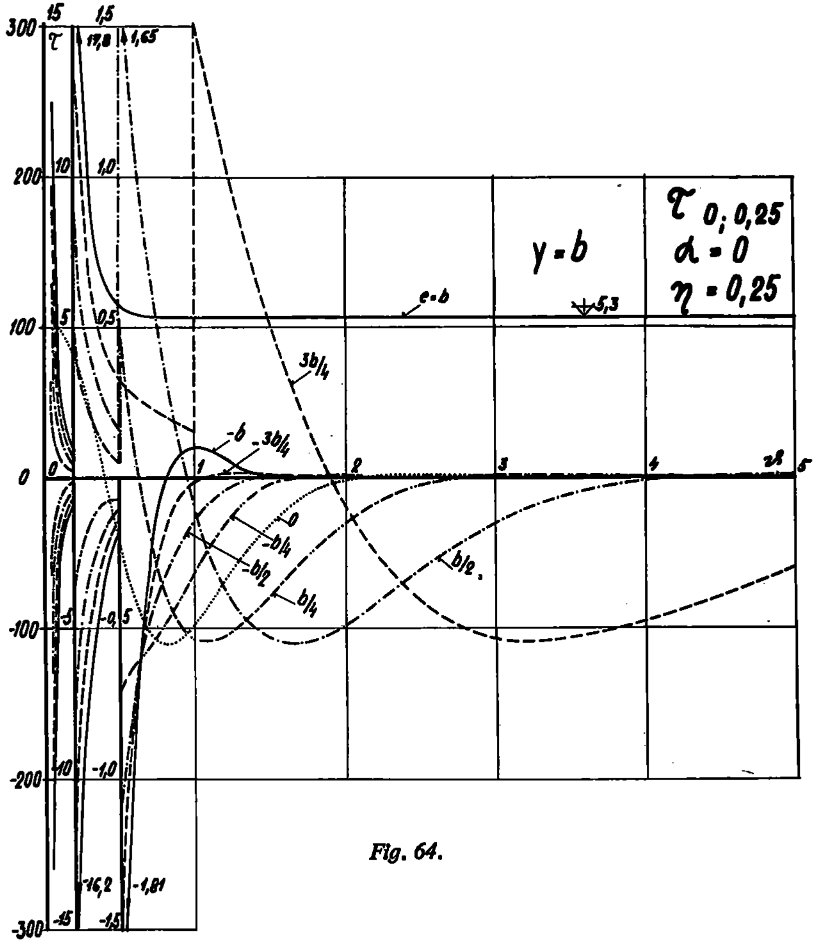
y = b
τ 0 ; 0,25
α = 0
η = 0,25
e = b
3b/4
-b
-3b/4
0
-b/4
-b/2
b/4
b/2
17,8
1,65
-16,2
-1,81
5,3

Fig. 64.

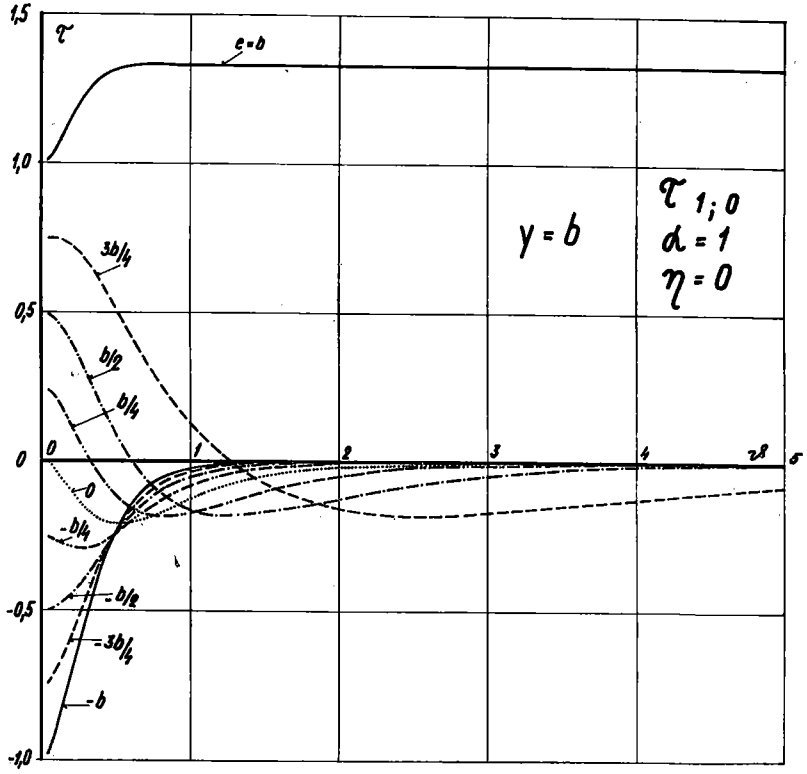
τ
e=b
3b/4
b/2
b/4
0
-b/4
-b/2
-3b/4
-b
y = b
τ 1; 0
α = 1
η = 0
1,5
1,0
0,5
0
-0,5
-1,0
0
1
2
3
4
28
s

Fig. 65.

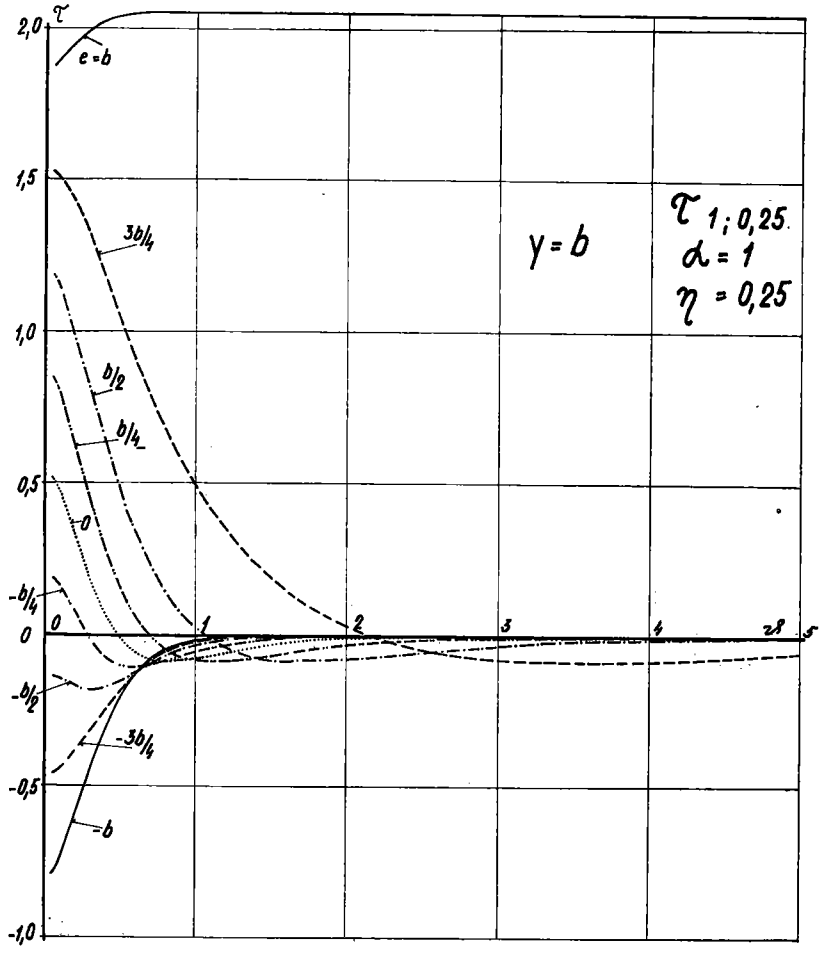
τ
e=b
3b/4
b/2
b/4
0
-b/4
-b/2
-3b/4
-b
y = b
τ 1; 0,25
α = 1
η = 0,25
2,0
1,5
1,0
0,5
0
-0,5
-1,0
0
1
2
3
4
28
s

Fig. 66.

In the case of a true orthotropic slab we should, naturally, obtain $M_{PT} = -M_{PT}$, since it is here $\gamma_T = \gamma_P$.

For the case *of a load harmonical in the X-direction, while uniform in the Y-direction* we find, similarly

$$(74) \qquad (M_{TP} - M_{PT})^o = \sum \frac{2p_m^0}{\pi^2 m^2} \frac{lb}{\vartheta} (\alpha - \eta) [\tau^0(y)_m] \cos \frac{m\pi x}{l},$$

where the dimensionless parameter τ^0 is given by the relation

$$(75) \qquad \tau^0(y)_m = \eta \sqrt{\left(\frac{1+\varepsilon}{2}\right)} \left[(A_m^{0\prime} M_{ym} - \bar{B}_m^{0\prime} N_{ym}) - \sqrt{\left(\frac{1-\varepsilon}{1+\varepsilon}\right)} (A_m^{0\prime} N_{ym} + \right.$$

$$\left. + \bar{B}_m^{0\prime} M_{ym}) + (A^{0\prime} O_{ym} - \bar{B}_m^{0\prime} P_{ym}) + \sqrt{\left(\frac{1-\varepsilon}{1+\varepsilon}\right)} (A_m^{0\prime} P_{ym} + \bar{B}_m^{0\prime} O_{ym}) \right].$$

For $m = 1$ the numerical values of τ^0 are given by the graphs shown in the figures 67–68, where they are plotted for $\alpha = 0$, $\alpha = 1$, and for $\eta = 0{\cdot}25$, as dependent on the parameter ϑ, which represents here the independent variable.

Fig. 67.

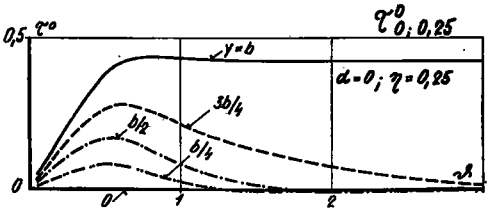

Fig. 68.

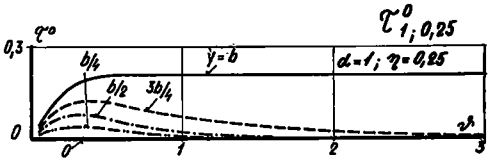

8. SHEAR FORCES AND SUPPORT REACTIONS FOR MAIN BEAMS

The shearing forces Q_T (for the X-direction) and the corresponding support reactions, $\bar{Q}_T$ are given by the third partial derivative of the function $w(x, y)$ as given above, by the expressions (11) and (12). For the *case of a harmonic line load*, we obtain – on introducing the dimensionless parameters K and μ according to (46) and (65) – after some transformations the following relations

$$(76) \qquad Q_T = \sum \frac{p_m l}{2bm} \left\{ K(y)_m + \left(\frac{\gamma_P}{\sqrt{(\varrho_T \varrho_P)}} + \eta \right) \mu(y)_m \right\} \cos \frac{m\pi x}{l}$$

and

$$\bar{Q}_T = \sum \frac{p_m l}{2bm} \{K(y)_m + (2\varepsilon - \eta)\,\mu(y)_m\} \cos \frac{m\pi x}{l}. \tag{77}$$

When the *load is harmonically distributed along X, while it is uniform along Y (that is uniform in the lateral direction)*, we find in a manner similar as above

$$Q_T^0 = \sum \frac{l p_m^0}{\pi m} \left\{1 + K^0(y)_m - \left(\frac{\gamma_P}{\sqrt{(\varrho_T \varrho_P)}} + \eta\right) \mu^0(y)_m\right\} \cos \frac{m\pi x}{l} \tag{78}$$

and

$$\bar{Q}_T^0 = \sum \frac{l p_m^0}{\pi m} \{1 + K^0(y)_m - (2\varepsilon - \eta)\,\mu^0(y)_m\} \cos \frac{m\pi x}{l}. \tag{79}$$

Here the dimensionless parameters K^0 and μ^0 are given by the above expressions (58) and (67), respectively.

9. TRANSVERSE SHEAR FORCES

For the cross beams, bending in the lateral direction Y, the shearing forces as defined by the third derivative of the deflection $w(x, y)$, are given by equation (11). For *the case of a harmonic line load* we perform the indicated operations to obtain after some simplifications – the following expression

$$Q_P = p_m \left\{\varkappa(y)_m + \frac{1}{4}\left(\eta + \frac{\gamma_T}{\sqrt{(\varrho_T \varrho_P)}}\right) \tau(y)_m\right\} \sin \frac{m\pi x}{l}. \tag{80}$$

Here the factor $\tau(y)_m$ is defined as in (72), while the newly introduced dimensionless parameter $\varkappa(y)_m$ is given by the formula

$$\begin{aligned} \varkappa(y)_m = -\frac{1}{4}\Bigg[& (2\varepsilon - 1)\,(A'_m M_{\varphi m} + \bar{B}'_m N_{\varphi m}) - (2\varepsilon + 1)\sqrt{\left(\frac{1-\varepsilon}{1+\varepsilon}\right)}\,(A'_m N_{\varphi m} - \\ & - \bar{B}'_m M_{\varphi m}) - (2\varepsilon - 1)\,(C'_m O_{\varphi m} + \bar{D}'_m P_{\varphi m}) - \\ & - (2\varepsilon + 1)\sqrt{\left(\frac{1-\varepsilon}{1+\varepsilon}\right)}\,(C'_m P_{\varphi m} - \bar{D}'_m O_{\varphi m}) \pm \\ & \pm \left(\frac{2\varepsilon}{\sqrt{(1-\varepsilon^2)}} P_{|\varphi - \Psi| m} - 2 O_{|\varphi - \Psi| m}\right)\Bigg]. \end{aligned} \tag{81}$$

[1]) For $\eta = 0$ the parameter is identical with the original parameter introduced by Bareš [8, 164]; thus

$$[\varkappa(y)_m]_{\eta=0} \equiv \varkappa(y)_m^{\mathrm{BAR}}.$$

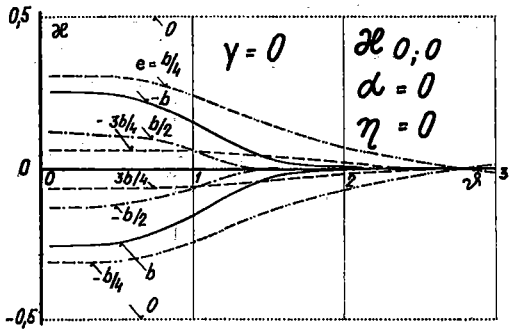

Fig. 69.

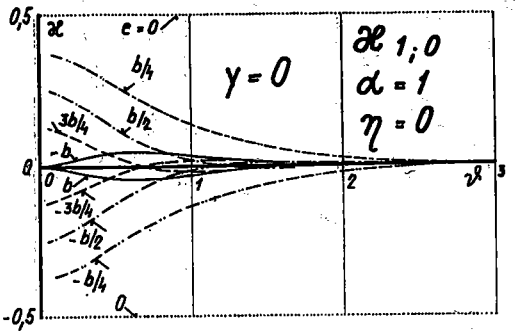

Fig. 71.

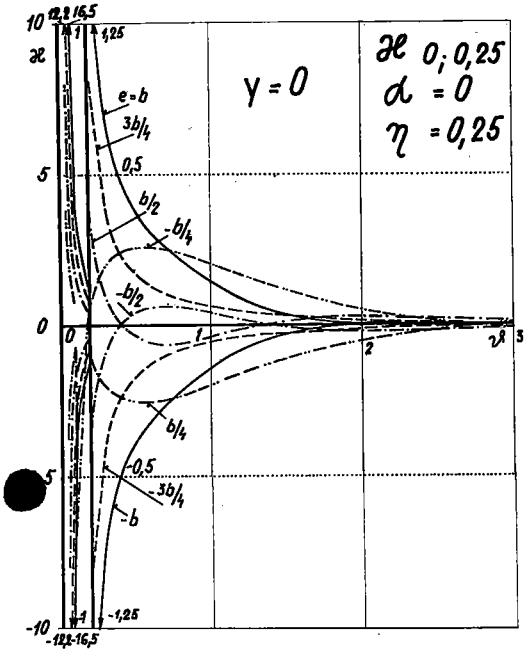

Fig. 70.

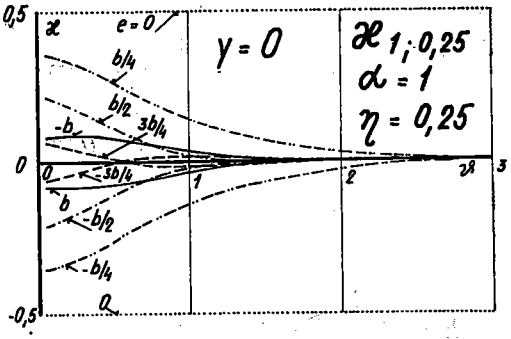

Fig. 72.

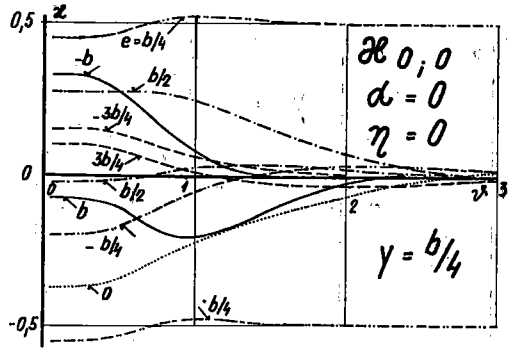

Fig. 73.

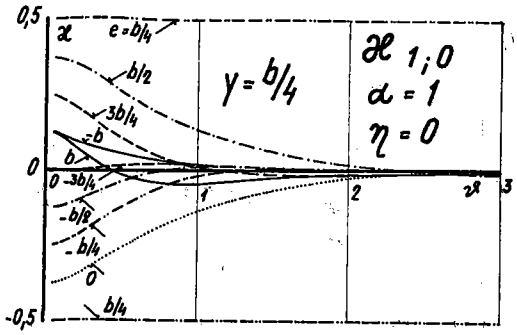

Fig. 75.

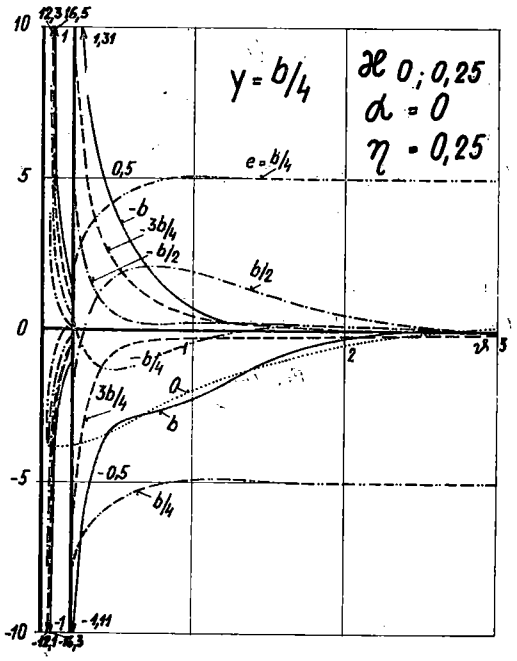

Fig. 74.

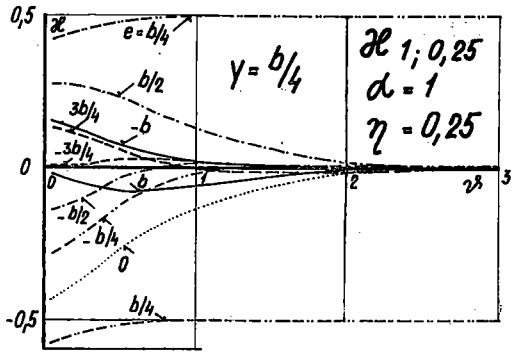

Fig. 76.

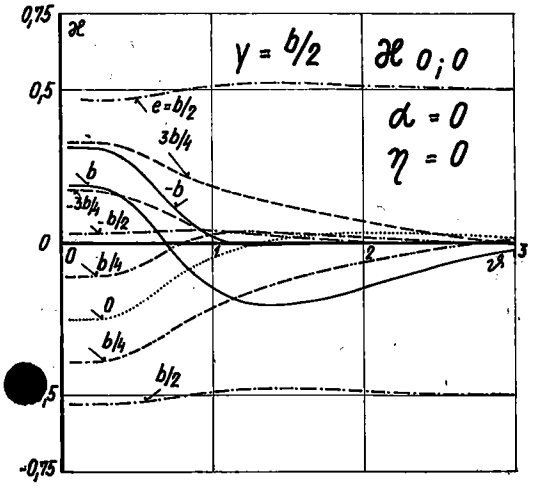

Fig. 77.

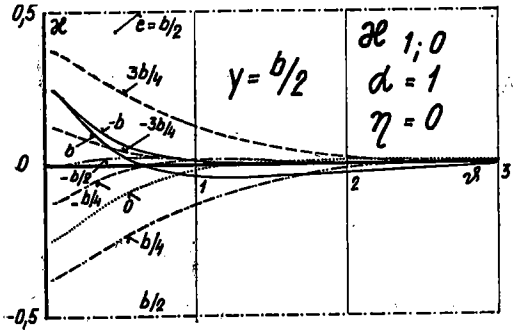

Fig. 79.

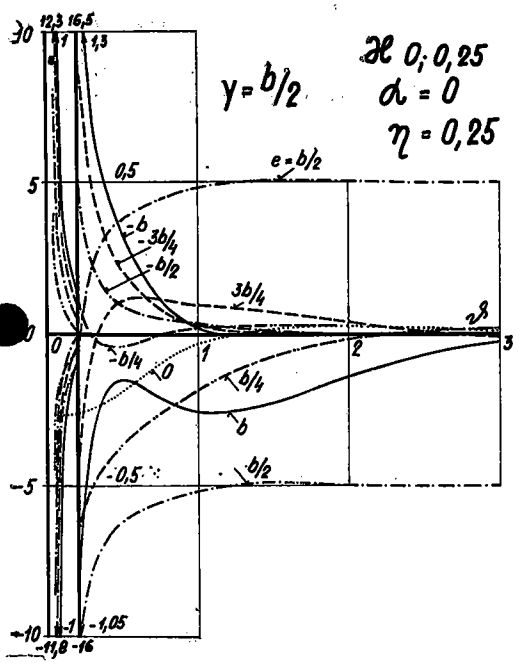

Fig. 78.

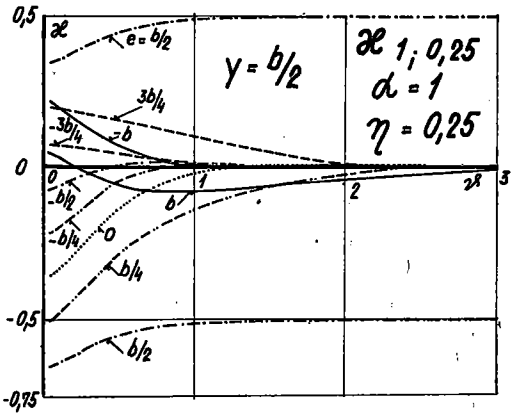

Fig. 80.

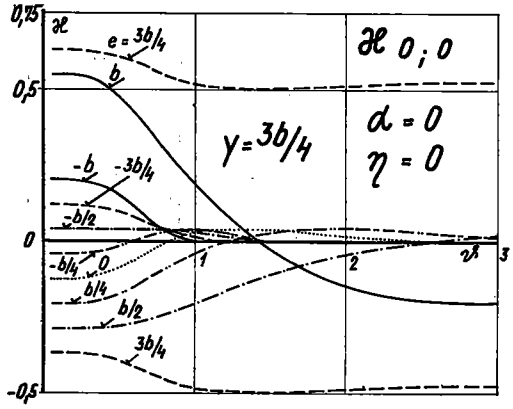

Fig. 81.

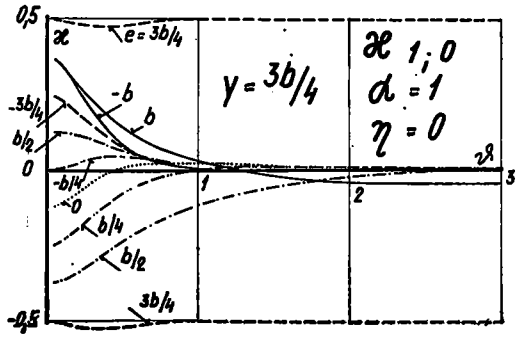

Fig. 83.

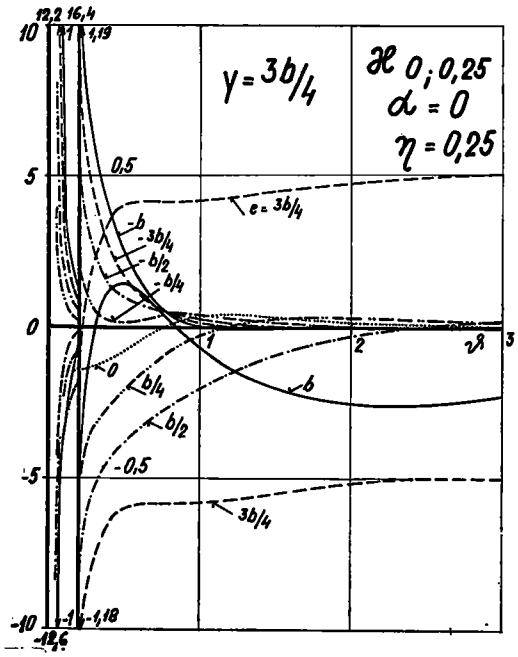

Fig. 82.

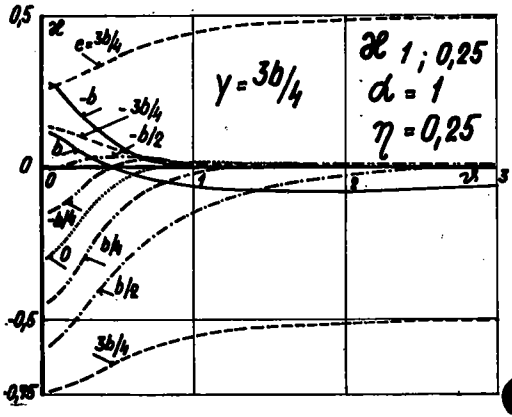

Fig. 84.

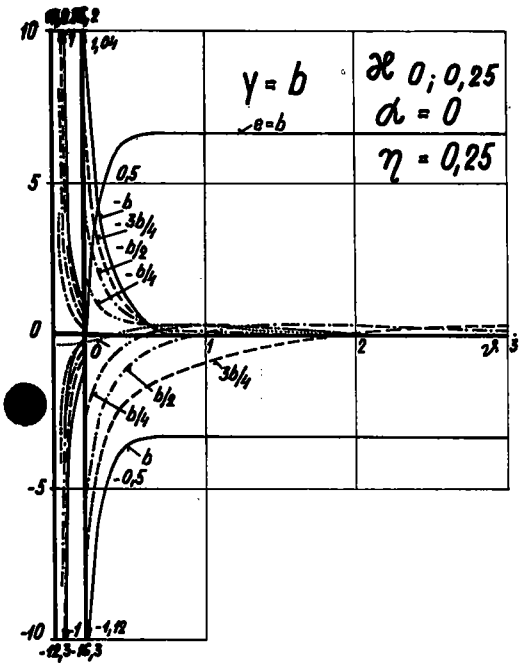

Fig. 85.

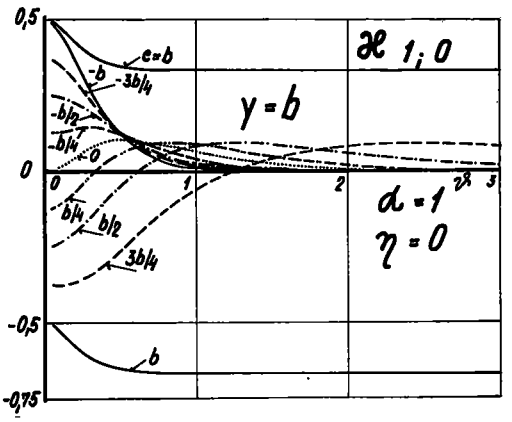

Fig. 86.

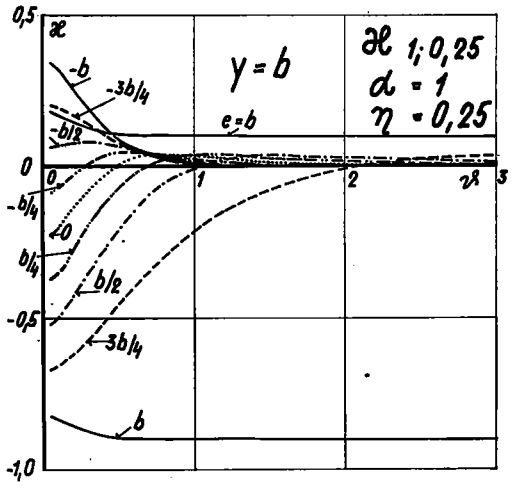

Fig. 87.

The last term on the right side of (81) is positive if $\varphi < \psi$, while for $\psi < \varphi$ it is negative. Graphical representation of the parameter $\varkappa \equiv \varkappa(y)_1$ is shown in the figures 69 to 87, where the values of $\varkappa$ are plotted against the independent variable ϑ; the graphs have been drawn for $\alpha = 0$, $\alpha = 1$, and for $\eta = 0$, or $\eta = 0{\cdot}25$, and for various values of φ and ψ.

For the particular *case of a load of harmonic distribution along X, and uniform in the Y-direction* (*lateral*), we obtain, similarly

$$(82) \qquad Q_P^0 = \sum \frac{p_m^0 b}{\pi m \vartheta} \left\{ \left[\eta + \frac{\gamma_T^0}{\sqrt{(\varrho_T \varrho_P)}} \right] \tau^0(y)_m - \varkappa^0(y)_m \right\} \sin \frac{m\pi x}{l},$$

where $\tau^0(y)_m$ is defined by (75), while the dimensionless parameter $\varkappa^0(y)_m$ has the

following value

$$(83)\qquad \varkappa^0(\dot{y})_m = \eta\sqrt{\left(\frac{1+\varepsilon}{2}\right)}\Big[-(1-2\varepsilon)\,(A_m^{0\prime}M_{\varphi m} - \bar{B}_m^{0\prime}N_{\varphi m}) -$$

$$-(1+2\varepsilon)\sqrt{\left(\frac{1+\varepsilon}{1-\varepsilon}\right)}(A_m^{0\prime}N_{\varphi m} + \bar{B}_m^{0\prime}M_{\varphi m}) -$$

$$-(1-2\varepsilon)\,A_m^{0\prime}O_{\varphi m} - \bar{B}_m^{0\prime}P_{\varphi m}) + (1+2\varepsilon)\sqrt{\left(\frac{1-\varepsilon}{1+\varepsilon}\right)} \times (A_m^{0\prime}P_{\varphi m} + \bar{B}_m^{0\prime}O_{\varphi m})\Big].$$

For $\alpha = 0$ and for $\alpha = 1$, (while $\eta = 0{\cdot}25$) the values of $\varkappa^0 \equiv \varkappa^0(y)_1$ are plotted vers the independent variable ϑ, for various values of φ in the graphs in the figures 88–89.

Fig. 88.

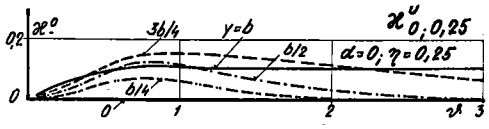

Fig. 89.

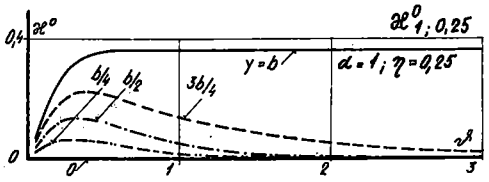

Along the edges $y = \pm b$ the latter equations (80) and (82) do, naturally, not furnish the proper values of the transverse shear forces. This follows from Kirchhoff's simplification, that is from the use of corrected values of the shear forces at the edges, instead of the proper twisting moments, as explained above (Chapter 2.4). The proper expressions for the shear forces at the edges $y = \pm b$ are to be obtained by means of equation (12), on substituting the pertinent derivatives of $w(x, y)$ according to Eq. (45) for harmonic line load, while for the case of a load harmonically distributed along X, and uniform along Y (i.e. across the width), we have to employ Eq. (57a). In the indicated manner we obtain

$$(84)\qquad \bar{Q}_P = \sum p_m \left\{\frac{1}{4}(2\varepsilon - \eta)\,\tau(y)_m + \varkappa(y)_m\right\} \sin\frac{m\pi x}{l}$$

and similarly

$$(85)\qquad \bar{Q}_P^0 = \sum p_m^0 \{(2\varepsilon - \eta)\,\tau^0(y)_m - \varkappa(y)_m\} \sin\frac{m\pi x}{l}.$$

Since the whole solution has been developped so as to meet the boundary condition along a free edge where the shear force must – of necessity – be equal to zero for any arbitrary sort of load, the latter two equations (84) and (85) serve mainly as a convenient check upon the calculation. Therefore at $y = \pm b$ and for $-b \leqq e \leqq \frac{3}{4}b$ the member in brackets on the right hand side of Eq. (84) or (85) (respectively), is equal to zero, while for $e = b$ it is equal to one.

References

[1] Bareš R., Compléments à la méthode Guyon-Massonnet de calcul des ponts à poutres multiples, Ann. des Travaux Publics de Belgique 116, 1963.

[2] Bareš, R.: Ohybové a torsní tuhosti tvarově ortotropní plošné konstrukce, Stavebnický časopis, 1974, No. 4.

[3] Bareš, R., Machan, P.: Přesný výpočet tvarově ortotropních desek, Rozpravy ČSAV, TV, No. 4, 1962.

[4] Bareš, R., Massonnet Ch.: Le calcul des grillages de poutres et dalles orthotropes selon la méthode Guyon-Massonnet-Bareš, DUNOD, Paris, 1966.

[5] Girkmann K.: Flächentragwerke, 5th Ed., Wien, 1959.

[6] Guyon, Y.: Calcul des ponts larges à poutres multiples solidarisées par des entretoises, Ann. des Ponts et Chaussées de France, 1946, pp. 553—612.

[7] Guyon, Y.: Calcul des ponts-dalles, Ann. des Ponts et Chaussées de France, 1949, pp. 555—589, 683—718.

[8] Hetenyi, M.: Beams on elastic foundation, Univ. of Michigan Press, 1946.

[9] Huber M. T., Ueber die genaue Berechnung einer orthotropen Platte, Bauingenieur 7, 1925, p. 7.

[10] Kirchhoff G. J., Math. (Crelle) 40, 1850, p. 51.

[11] Massonnet, Ch.: Méthode de calcul des ponts à poutres multiples tenant compte de leur résistance à la torsion, Memoires A.I.C.P. 10, 1950, pp. 147—182.

[12] Massonnet, Ch.: Compléments à la méthode de calcul des ponts à poutres multiples, Ann. Trav. Publ. de Belgique 107, 1954, pp. 680—748.

[13] Massonnet, Ch.: Contribution au calcul des ponts à poutres multiples, Ann. Trav. Publ. de Belgique 103, 1950, pp. 377—422, 749—796, 927—964.

ANALYSIS OF FORM-ORTHOTROPIC PLANE SYSTEMS BY THE METHOD OF DIMENSIONLESS PARAMETERS

PART 2

The analysis of form-orthotropic plane structures of the simple bridge type by means of the method of dimensionless parameters which, in turn, is based on the analogy with material orthotropy pertinent to slabs, enables us to obtain in a convenient manner all the internal force-components, that is the bending and the twisting moments, as well as the shear forces and support reactions. One of the dimensionless parameters required in the procedure has been defined previously (see Part 1), in connection with the definition of the deflection. The remaining three dimensionless parameters have been evaluated for the main (limiting) types of structures, and their values have been represented graphically, for the limit values of the torsional parameter α and of the parameter of contraction capability η, considering each time 45 combinations φ and ψ, as depending upon the variation of the parameter of lateral stiffness ϑ within the range 0 and 5·0.

The described method works with well defined dimensionless parameters of known numerical values (as given in the graphs); it will be found not only very expedient, but it will also furnish the means for numerical analysis of arbitrary, given degree of accuracy, for any structure of the given type for any given case of loading.

[Received April 10, 1973]

Ing. Richard Bareš, CSc., Institute of Theoretical and Applied Mechanics, Czechoslovak Academy of Sciences, Vyšehradská 49, 128 49 Praha 2 - Nové Město.